

Thermally activated and field dependent hole transport in poly(3-hexylthiophene)

Ranoo Bhargav^{1,2}, Asit Patra^{1,2,*}, Suresh Chand¹

¹Organic & Hybrid Solar Cells Group, Physics of Energy Harvesting Division and CSIR-Network of Institutes for Solar Energy, CSIR-National Physical Laboratory (CSIR-NPL), Dr. K. S. Krishnan Marg, New Delhi 110012, India

²Academy of Scientific and Innovative Research (AcSIR), CSIR-NPL Campus, Dr. K. S. Krishnan Marg, New Delhi 110012, India

*Corresponding author. Tel: (+91) 11-4560-8360; E-mail: apatra@nplindia.org

Received: 11 May 2015, Revised: 07 December 2015 and Accepted: 02 April 2016

ABSTRACT

Here, we investigate the hole transport mechanism in poly(3-hexylthiophene) (P3HT). First, ohmic contact has been established at indium tin oxide (ITO)/P3HT interface by molybdenum oxide (MoO_x) hole injection layer. Thickness of MoO_x layer is observed to play a crucial role with ohmic contact being observed even for 1 nm layer. However, device with less than 5 nm layer are found to be extremely unstable. A device with a 5 nm layer of MoO_x is found to be stable and ohmic injection at ITO/P3HT layer enabled to observe ohmic conduction at low voltages (< 3 V), trap free space charge limited conduction (SCLC) for > 3 V. At higher voltages, effect of field on charge carrier mobility is also observed. Observation of SCLC enabled us to directly evaluate the hole mobility in P3HT which is calculated to be 5.4×10^{-5} cm²/Vs. Conductivity is calculated from the low voltage region and found to be 6.85×10^{-8} S/cm. Temperature dependent mobility is used to study the charge transport behavior and it has been observed that mobility is thermally activated with an extremely low activation energy of 39 meV. Copyright © 2016 VBRI Press.

Keywords: Hole transport; *p*-type polymer; activation energy; field dependent mobility.

Introduction

Low cost organic semiconducting devices such as organic photovoltaics (OPVs) and organic light emitting diodes (OLEDs) have been intensively investigated as a viable replacement for their high cost inorganic counterparts [1-5]. The benefits of OPV include ease of fabrication, variety of options for semiconducting absorbing layer, ultra-low thickness of the cell which makes it useful to use near field effects originated from plasmon etc [6-10]. Several materials have been investigated as the semiconducting absorbing layers in OPVs. Generally, this layer is composed of a polymer blend of donor and acceptor materials [11]. Several donor materials have been utilized which include poly[2-methoxy-5-(2-ethylhexyloxy)-1,4-phenylenevinylene] (MEH-PPV), poly(3-hexylthiophene) (P3HT), poly[*N*-9'-heptadecanyl-2,7-carbazole-alt-5,5-(4',7'-di-2-thienyl-2',1',3'-benzothiadiazole)] (PCDTBT) etc., while the acceptor materials are generally derivatives of fullerene, inorganic quantum dots etc [6, 7, 11, 12].

Efficiency of OPV depends on the hole transport in the donor material [1-6]. Hole transport studies have been performed using time of flight (TOF) method for several materials used in OPVs [13, 14]. The used thickness in TOF samples (~ 1 – 10 μm) is very high in comparison to the practical OPVs and it has already been inferred by several authors that the charge transport in organic semiconductor is highly dependent on the thickness [15, 16]. Therefore, the charge transport studies performed

on thin samples (~100 nm) are of more practical use. These studies are generally performed by measuring the current density-voltage (J-V) characteristics at different temperatures and have been found very useful in extracting several parameters which decides the charge transport in organic semiconductor [17-20]. However, the hole transport studies have been limited due to non-ohmic injection into the organic materials from indium tin oxide (ITO) anode [21, 22]. The reason behind the non-ohmic injection is low work function of ITO, which is generally increased by oxygen plasma treatment. Alternatively, several interface layers can be utilized to support ohmic injection into organic solar cells (OSCs) [23-26]. Most widely used interface layers are polymer (poly(3,4-ethylenedioxythiophene): poly(4-styrenesulfonate) (PEDOT: PSS)) [23], metal oxides (MoO₃, WO₃) etc. [25, 26]. Out of these choices PEDOT: PSS and MoO₃ are mostly used in organic electronic devices for improving the hole injection from ITO. Improved injection using PEDOT: PSS requires its relatively higher thickness (> 30 nm) and also PEDOT: PSS leads to degradation of the device due to the presence of acid. Additionally, PEDOT: PSS is hydrophilic in nature. In contrast, 5-10 nm of MoO₃ has been found to improve the hole injection from ITO as studied in OLEDs and found to be relatively stable. Therefore, MoO₃ is a relatively better choice for study of hole transport in OSCs.

MoO₃ has previously been used for the study of hole transport in poly(9,9-dioctylfluorene) and ohmic injection

was observed by 15 nm thin layer of MoO₃ [27]. The ohmic injection in this case has led to the direct measurement of charge carrier mobility. Therefore, MoO₃ interface layer can be used efficiently to study the hole transport in the materials used as donors in case of OPVs. P3HT is the widely used donor material for OPVs and its hole mobility has already been measured using a TOF method [28]. Several methods have been employed for the hole transport studies in P3HT which includes TOF [28], field effect transistors [29], charge extraction by linearly increasing voltage etc. [30].

However, the complete understanding of the hole transport mechanism in P3HT is required which can be achieved by first establishing an ohmic contact with the electrode. Since the thickness of MoO_x is a crucial parameter which decides its injection properties with hole injecting electrodes, it needs to be optimized for establishing the ohmic contact. Further, for the complete understanding of hole transport, temperature dependent J-V characteristics can be measured on the hole only devices of P3HT. Qualitative analysis of these J-V characteristics can thus provide a detailed understanding of the hole transport mechanism. Here, we have established an ohmic contact with P3HT by optimizing the thickness of MoO_x. After establishing the ohmic contact, temperature dependent J-V studies are performed and the data is analyzed in order to obtain various hole transport related parameters.

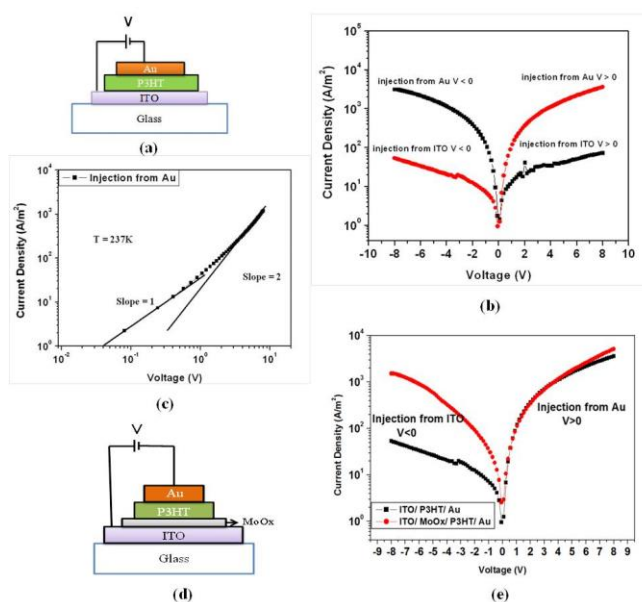


Fig. 1. (a) Device structure, (b) J-V characteristics for hole only device in the voltage range of -8 to 8 V for both polarities, (c) The J-V characteristics in semi log for the hole only device with ITO/P3HT/Au, (d) Device Structure with MoO_x as interface layer and (e) comparison of J-V characteristic with and without MoO_x (1 nm) as interface layer.

Experimental

Materials

Chemicals and solvents were purchased from Sigma-Aldrich and Alfa Aesar and used without further purification.

Device fabrication

The hole only device was fabricated on a cleaned ITO coated glass substrate with sheet resistance of 20 ohm/sq. The substrate was cleaned sequentially in distilled water, acetone, trichloroethylene and isopropanol for 20 minutes each in an ultrasonic bath. Cleaned substrates were then transferred into a vacuum chamber where MoO_x was deposited at a base pressure of 9.8x10⁻⁶ torr. P3HT was then deposited over MoO_x coated substrates by spin coating its solution of 20 mg/ml in chlorobenzene at a rotation speed of 1000 rpm. Samples were then heated in an inert atmosphere at a temperature of 120 °C to remove the residues of solvents. Samples were then again transferred into a vacuum chamber where the counter gold electrode was deposited at a base pressure of 9.8x10⁻⁶ torr.

Characterization

J-V characteristics were measured in a homemade cryostat connected with a temperature controller using Keithley 2420 source meter. Surface morphology of MoO₃ films were measured using an atomic force microscope model number NT-MDT Solver Pro.

Results and discussion

Fig. 1(a, b) demonstrates the device structure for hole only devices and the J-V characteristics for the device without the interface layer. The devices are considered solely to conduct the hole current due to the large potential barrier for electrons (~ 1.2 to 1.6 eV) from the Fermi level of ITO (4.8 eV to 5.1 eV) to the LUMO of P3HT. It can be seen in **Fig. 1(b)** that the current density is lower when the holes are injected from ITO in comparison to when they are injected from gold. The difference in the current density is nearly two orders of magnitude. This indicates a poor injection of holes from ITO in comparison to gold. This may be attributed to the potential barrier at the ITO/P3HT interface. This potential barrier can vary from 0.5 eV to 0.1 eV according to the work function of ITO, however, this barrier was found to be greater than the theoretical value due to the dipole formation at this interface. The current was found to have a higher value when we inject the hole from Au electrode due to the compatibility of Au work function (5.1 eV) with the highest occupied molecular orbital (HOMO) of P3HT. We have taken the measurements by changing the polarity and found the similar results in both the cases.

We have performed the analysis by taking the injection from gold. **Fig. 1(c)** shows the J-V characteristics when the holes are injected from Au electrode. Current density shows a nonlinear behavior with voltage. It was found to follow ohms law in the low voltage region (< 3V) and quadratic dependence at higher voltages (> 3V). The observed ohms law in the low voltage regime can be ascribed as due to the doping of P3HT by background impurities. While, the quadratic dependence in the higher voltage region is due to the formation of the space charge region as a consequence of low conductivity of P3HT. We have calculated the conductivity by using ohm's law,

$$J = \sigma E \quad (1)$$

where, J is the current density, σ the conductivity and $E = \frac{V}{d}$ is the electric field. The calculated value was found to be 6.85×10^{-8} S/cm. The mobility has been calculated by using the Mott-Gurney law,

$$J = \frac{9}{8} \mu \epsilon \epsilon_0 \frac{V^2}{d^3} \quad (2)$$

where, μ is the mobility of holes in P3HT, ϵ the relative permittivity, ϵ_0 the permittivity of free space, V the applied voltage and d is the thickness of the active layer. The estimated mobility was found to be 5.4×10^{-5} cm²/Vs in the voltage range of 3-10 V at 237 K. Mobility is field independent in this voltage range.

Most of the devices use ITO/P3HT interface therefore it is required to obtain an ohmic injection at this interface. To serve the purpose, we have used MoO_x layer at this interface. **Fig. 1(d, e)** shows the schematic and the J-V characteristics of the interface modified hole only devices. From the figure it is clear that the current density increased by two orders of magnitude with the insertion of 1 nm MoO_x interface layer when the holes are injected from ITO. The current density thus became comparable to that when the holes are injected from gold. This may be attributed to the improved hole injection at this interface. This improvement is associated to the fact that a thin metal oxide layer at the ITO/P3HT interface improves the work function of ITO [31]. The work function of MoO_x is 5.3 eV and the HOMO of P3HT lies at 5.1 eV. MoO_x form efficient hole injection and collection contact with P3HT. During the experiments, we found that the devices with 1 nm MoO_x layer were not stable and the current drops down to 2-3 orders of magnitude in 5 min. This may be due to the non-uniform coverage of ITO substrates for 1 nm or less thickness of MoO_x layer.

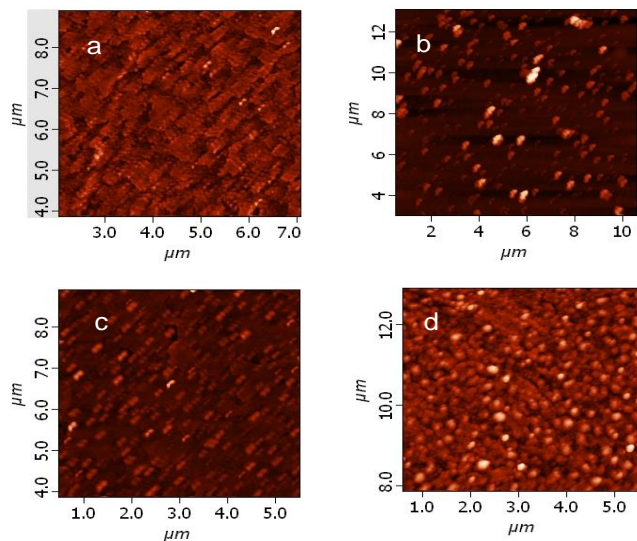


Fig. 2. AFM image of (a) 1 nm, (b) 3 nm, (c) 5 nm and (d) 7 nm MoO_x layers deposited on ITO coated glass substrate.

To confirm this we have performed the morphological studies using atomic force microscopy (AFM). **Fig. 2(a-d)**

shows the AFM images for 1, 3, 5 and 7 nm MoO_x layer deposited on ITO coated glass substrate. It is evident from the figure that the coverage for 1 and 3 nm layers is extremely low which has increased for 5 and 7 nm layers.

It is very important to optimize the thickness of injection layer to get a stable device. To serve the purpose, we have optimized the thickness of MoO_x layer by varying it as 3, 5 and 10 nm. The variation in current density was found within the experimental error. Therefore, further analysis is performed on a device with 5 nm MoO_x interface layer and J-V characteristics have been measured at different temperatures.

It is very important to optimize the thickness of injection layer to get a stable device. To serve the purpose, we have optimized the thickness of MoO_x layer by varying it as 3, 5 and 10 nm. The variation in current density was found within the experimental error. Therefore, further analysis is performed on a device with 5 nm MoO_x interface layer and J-V characteristics have been measured at different temperatures.

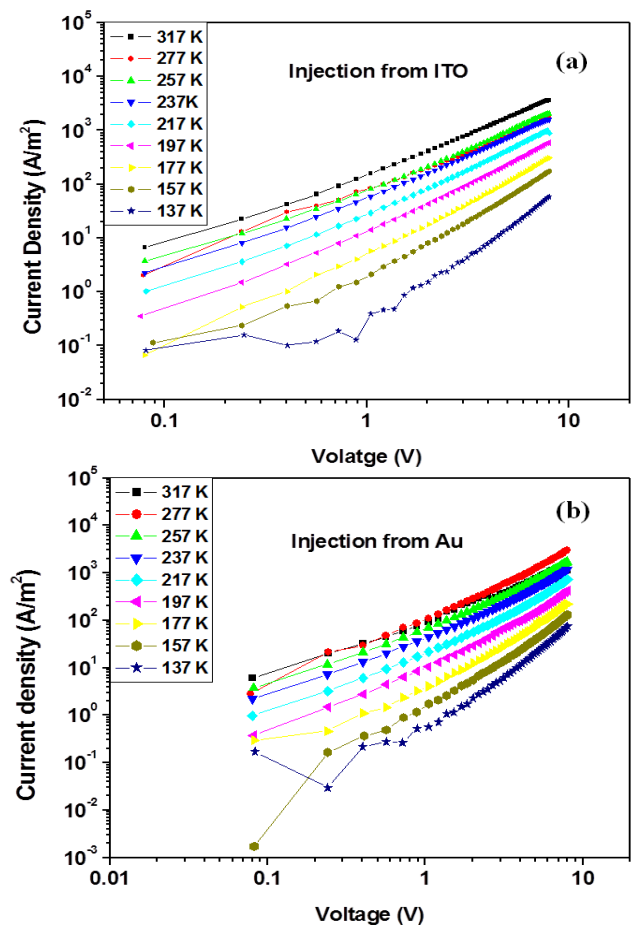


Fig. 3. J-V Characteristic at different temperatures of the device with 5 nm MoO_x interface layer (a) Injection from ITO (ITO +ve) (b) Injection from Au (Au +ve).

Further, to investigate the effect of this MoO_x interface layer, we have measured the J-V characteristics at different temperatures. **Fig. 3(a, b)** depict the J-V characteristics of the hole only device for injection from ITO and gold, respectively. It is evident from the figure that the current

density decreases with the decrease in temperature. It is also clear that the insertion of 5 nm MoO_x layer makes the injection of holes from ITO equivalent to the injection of holes from Au. Since the current density in the hole only device is originated from the combined effect of free and space charge carrier density, we have fitted the experimental J-V characteristics by using the equation

$$J = ne\mu \frac{V}{d} + \frac{9}{8} \mu \epsilon \epsilon_0 \frac{V^2}{d^3} \quad (3)$$

Here, n is the carrier concentration, μ the mobility of holes, V the applied voltage, d the thickness of active layer, ϵ the dielectric constant and ϵ_0 the permittivity of the free space. Eq. 3 includes the contribution by free charge carrier density (first term on the right hand side) and space charge carrier density (second term on the right hand side).

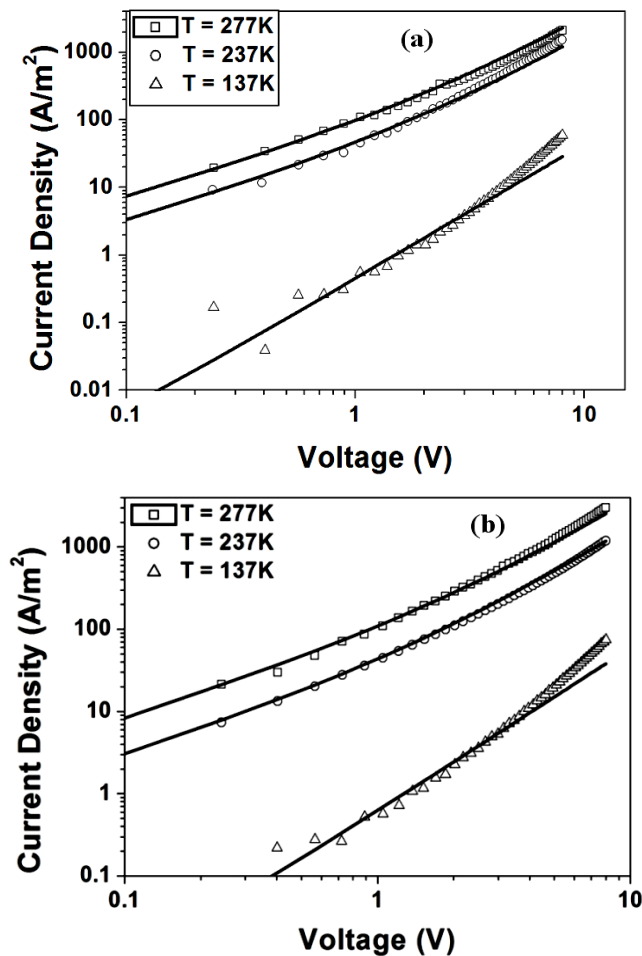


Fig. 4. Experimental (data points) and theoretical fitting (solid lines) for the hole only device for injection from (a) ITO and (b) Au side.

Fig. 4(a, b) depicts the experimental and theoretically fitted J-V characteristics for hole only device with injection from ITO and Au, respectively. It can be seen from the Fig. 4. that experimental data is excellently fitted Eq. 3 at all operating voltages. At low voltages, the contribution from free carrier density is dominant over that from the space charge density as reflected by close to the unity slope observed at low voltage. As the voltage increases, the slope

increases and reaches to the value of two which implicate the dominant mechanism to be space charge limited conduction. As the temperature decreases, the contribution from free carrier density start to decrease due to the reason of free carriers are thermally generated. At very low temperature (at 157 K), this contribution becomes negligible and the slope of 2 is observed right from the low voltage range. Second notable point from the Fig. 4 is the deviation of experimental data from the theoretically fitted one at higher voltages and the deviation being increased with the decrease in temperature (clearly visible at 137 K). The reason for this deviation is the electrical field dependence of mobility in organic semiconductors. Generally, an exponentially increasing pattern of mobility has excellently been found to explain the field dependence of the charge carrier mobility. This exponentially increasing term ($\mu = \mu_0 \exp(\beta\sqrt{F})$) (often referred as Poole-Frenkel type dependence) with μ_0 and β being the fitting parameters is substituted in place of mobility in Eq. 3. Fig. 5(a, b) show the fitted J-V curve at 137 K and for reference the theoretical curve using field independent mobility is also shown in the same figure.

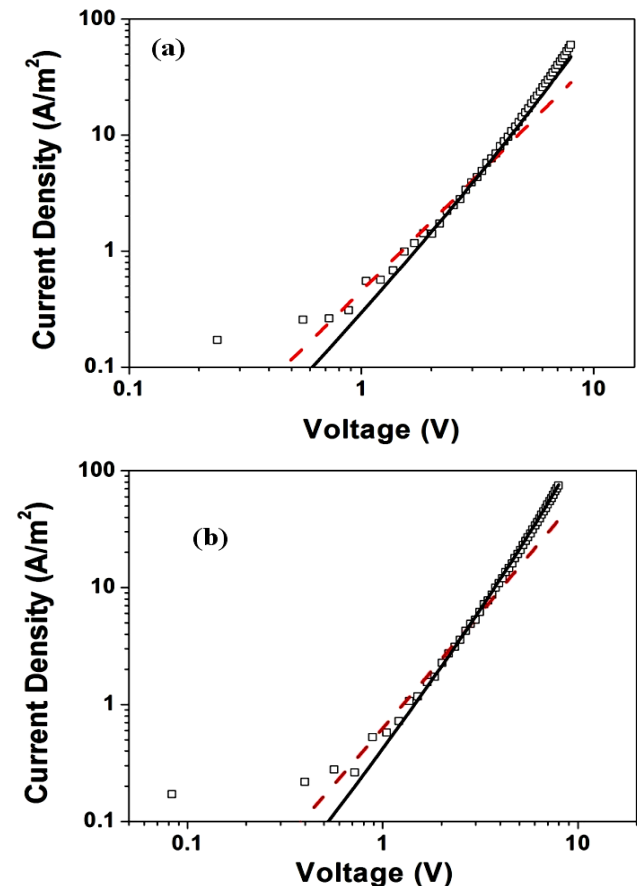


Fig. 5. Experimental data and theoretical fitting without field dependent mobility (dashed line) and with field dependent mobility (solid line) for the hole only device with injection from (a) ITO side (b) Au side) at 137 K.

It is evident from the Fig. 5 that the experimental data is better fitted with field dependent mobility. μ_0 and β are temperature dependent terms which are estimated from the

fitting of experimental J-V curves at different temperature and are plotted in Fig. 6(a). μ_0 decreases with temperatures while β shows an increasing pattern. A similar pattern has already been reported by other groups in case organic semiconductors.

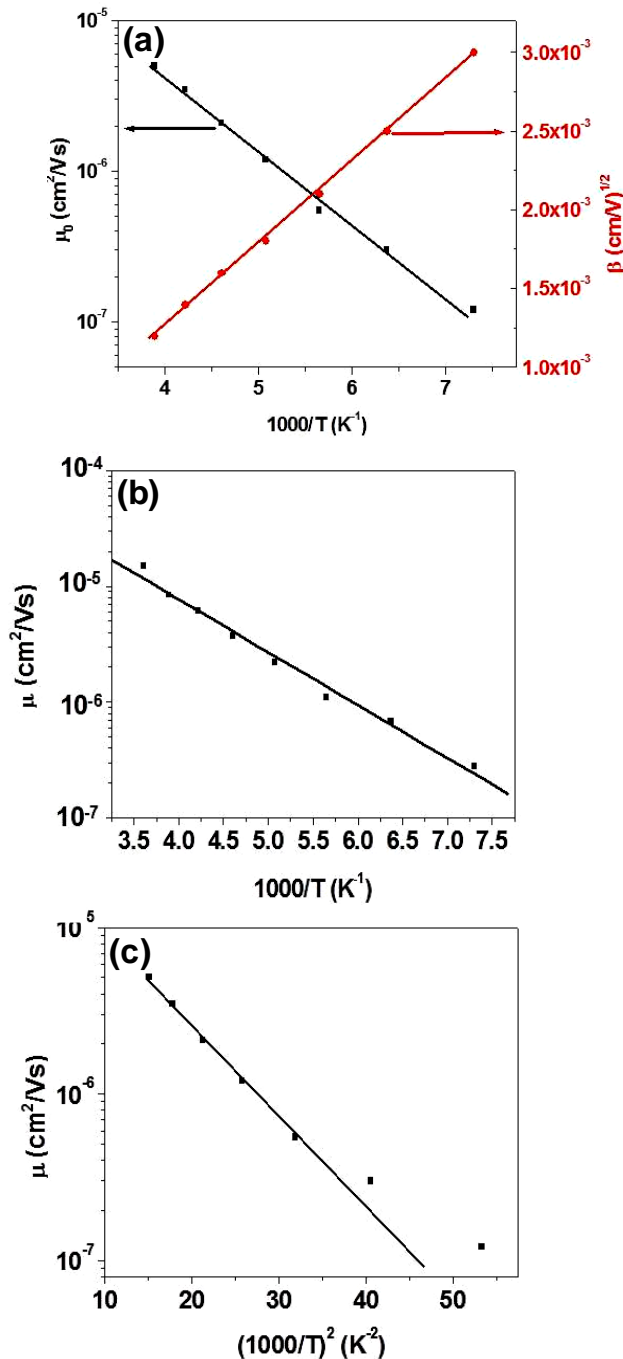


Fig. 6. (a) Values of μ_0 and β used for fitting the experimental data using field dependent mobility as a function of $1000/T$. Mobility as a function of (b) $1000/T$ and (c) $(1000/T)^2$ for hole only device.

Mobility is then estimated at different temperatures using the theoretical fitting of the experimental data. Generally, the mobility in organic semiconductors is explained using two models describing the mobility as either thermally activated or disordered. In case of thermally activated mobility, the dependence with temperature is linear to $1/T$

while in case of disordered it is $(1/T)^2$. To identify the dependence of the mobility in the case of our system, mobility is plotted in Fig. 6(b, c) as a function of $1000/T$ and $(1000/T)^2$. It is evident from the Fig. 6 that the mobility follows linear dependence with $1000/T$ which implicates that in our experimental system the mobility is thermally activated ($\propto \exp\left(-\frac{\Delta E}{kT}\right)$), where ΔE is the activation energy which is estimated to be 39 meV by using the slope of mobility vs $1000/T$ curve. Generally, the mobility in organic semiconductor is disordered type and described by a Gaussian function, which originates the $(1000/T)^2$ dependence. However, in most of the practical system $1000/T$ dependence is observed. The reason may that the tail state of Gaussian distributed energy states can be considered as an exponentially distributed one which originates the $1000/T$ dependence of mobility. Therefore, the $1000/T$ dependence implicates the charge carrier conduction being dominated by the tail energy states and the similar dependence in our system infers that the charge carrier conduction in P3HT is dominated by tail energy level states. The estimated activation energy is extremely low and is very close to room temperature thermal energy (~ 26 meV) which favors the use of P3HT as a hole transporting donor.

Conclusion

In conclusion, we have studied the hole transport in P3HT. First, ohmic contact from ITO has been established by optimizing the thickness of MoO_x . It is observed that the injection improves by even a 1 nm layer of MoO_x , however the device with less than 5 nm layer is found to be highly unstable. This has been attributed to the less coverage of MoO_x and is observed from morphological images captured from AFM 5 nm layer of MoO_x has been found to be an efficient injection layer to provide an ohmic contact at ITO/P3HT interface. J-V characteristics are then performed on the hole only devices as a function of temperature. Carrier mobility is extracted as 5.4×10^{-5} cm^2/Vs at 237 K and found comparable to that observed from TOF method. Temperature dependent measurements were then analyzed using SCLC model with including a field dependent mobility. Mobility and its field dependence was extracted by fitting of the experimental data. Mobility is found to follow the $1/T$ dependence which indicated towards a thermally activated charge transport with activation energy of 39 meV. Charge transport is dominated by the tail energy states.

Acknowledgements

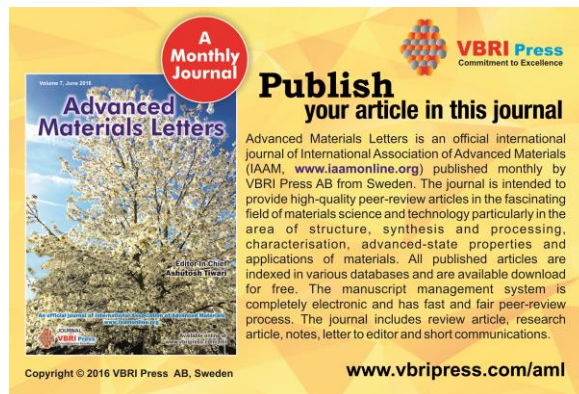
The authors are grateful to Dr Ritu Srivastava, CSIR-NPL, for help in AFM measurements. This work is financially supported by the CSIR-TAPSUN (NWP-54) program. R.B. gratefully acknowledged the receipt of her research fellowship from CSIR-TAPSUN (NWP-54) program.

Author's contributions

Conceived the plan: AP, RB. Performed the experiments: RB. Data analysis: RB.; Wrote the paper: RB, AP, SC. (RB, AP, SC are the initials of authors). Authors have no competing financial interests.

Reference

- Parida, B.; Iniyar, S.; Goic, R. *Renew. Sust. Ener. Rev.* **2011**, 15, 1625.
DOI: [10.1016/j.rser.2010.11.032](https://doi.org/10.1016/j.rser.2010.11.032)
- Inganäs, O.; Admassie, S. *Adv. Mater.* **2014**, 26, 830.
DOI: [10.1002/adma.201302524](https://doi.org/10.1002/adma.201302524)
- Pode R. *Adv. Mat. Lett.* **2012**, 2, 3.
- Yawalkar, P. W.; Dhoble, S. J. *Adv. Mat. Lett.* **2014**, 5, 678.
DOI: [10.5185/amlett.2014.amwc1033](https://doi.org/10.5185/amlett.2014.amwc1033)
- Bell, J.T.; Mola, G.T. *Physica B*, **2014**, 437, 63.
DOI: [10.1016/j.physb.2013.12.034](https://doi.org/10.1016/j.physb.2013.12.034)
- Mazzio, K. A.; Luscombe, C. K. *Chem. Soc. Rev.*, **2015**, 44, 78.
DOI: [10.1039/C4CS00227J](https://doi.org/10.1039/C4CS00227J)
- Yeh, N.; Yeh, P. *Renew. Sust. Ener. Rev.* **2013**, 21, 421.
DOI: [10.1016/j.rser.2012.12.046](https://doi.org/10.1016/j.rser.2012.12.046)
- Jeevadason, A. W.; Murugavel, K. K.; Neelakantan, M.A. *Renew. Sust. Ener. Rev.* **2014**, 36, 220.
DOI: [10.1016/j.rser.2014.04.060](https://doi.org/10.1016/j.rser.2014.04.060)
- Atwater, H. A.; Polman, A. *Nat. Mater.* **2010**, 9, 205.
DOI: [10.1038/nmat2866](https://doi.org/10.1038/nmat2866)
- Gan, Q.; Bartoli, F. J.; Kafafi, Z. H. *Adv. Mater.* **2013**, 25, 2385.
DOI: [10.1002/adma.201370107](https://doi.org/10.1002/adma.201370107)
- Kaur, N.; Singh, M.; Pathak, D.; Wagner, T.; Nunzi, J.M. *Syn. Met.* **2014**, 190, 20.
DOI: [10.1016/j.synthmet.2014.01.022](https://doi.org/10.1016/j.synthmet.2014.01.022)
- Sariciftci, N. S.; Braun, D.; Zhang, C.; Srdanov, V. I.; Heeger, A. J.; Stucky, G.; Wudl, F. *Appl. Phys. Lett.* **1993**, 62, 585.
DOI: [10.1063/1.108863](https://doi.org/10.1063/1.108863)
- Campbell, I. H.; Smith, D. L.; Neef, C. J.; Ferraris, J. P. *Appl. Phys. Lett.* **1999**, 74, 2809.
DOI: [10.1063/1.124021](https://doi.org/10.1063/1.124021)
- Choulis, S. A.; Kim, Y.; Nelson, J.; Bradley, D. D. C.; Giles, M.; Shkunov, M.; McCulloch, I. *Appl. Phys. Lett.* **2004**, 85, 3890.
DOI: [10.1063/1.1805175](https://doi.org/10.1063/1.1805175)
- Kumar, A.; Srivastava, R.; Tyagi, P.; Mehta, D.S.; Kamalasanan, M.N.; Reddy A.; Bhanuprakash, K. *Syn. Met.* **2010**, 160, 774.
DOI: [10.1016/j.synthmet.2010.01.019](https://doi.org/10.1016/j.synthmet.2010.01.019)
- Kumar, A.; Tyagi, P.; Reddy, M. A.; Malleshm, G.; Bhanuprakash, K.; Rao, V. J.; Kamalasanan, M. N.; Srivastava, R. *RSC Adv.*, **2014**, 4, 12206.
DOI: [10.1039/C3RA47215A](https://doi.org/10.1039/C3RA47215A)
- Tyagi, P.; Srivastava, R.; Kumar, A.; Tuli, S.; Kamalasanan, M. N. *Org. Elect.* **2013**, 14, 1391.
DOI: [10.1016/j.orgel.2013.02.034](https://doi.org/10.1016/j.orgel.2013.02.034)
- Parthasarathy, G.; Shen, C.; Kahn A.; Forrest, S. R. *J. Appl. Phys.* **2001**, 89, 4986-4992.
DOI: [10.1063/1.1359161](https://doi.org/10.1063/1.1359161)
- Poplavskyy, D.; Nelson, J. *J. Appl. Phys.* **2003**, 93, 341.
DOI: [10.1063/1.1525866](https://doi.org/10.1063/1.1525866)
- Brutting, W.; Berleb, S.; Muckl, A. G. *Org. Electron.* **2001**, 2, 1.
DOI: [10.1016/S1566-1199\(01\)00009-X](https://doi.org/10.1016/S1566-1199(01)00009-X)
- Melzer, C.; Koop, E.J.; Mihailetchi, V.D.; Blom, P. W. M. *Adv. Funct. Mater.* **2004**, 14, 865.
DOI: [10.1002/adfm.200305156](https://doi.org/10.1002/adfm.200305156)
- Chauhan, G.; Srivastava, R.; Kumar, A.; Rana, O.; Srivastava, P.C.; Kamalasanan, M.N. *Org. Elect.* **2012**, 13, 394.
DOI: [10.1016/j.orgel.2011.11.023](https://doi.org/10.1016/j.orgel.2011.11.023)
- de Jong, M. P.; van IJendoorn, L. J.; de Voigt, M. J. A. *Appl. Phys. Lett.* **2000**, 77, 2255.
DOI: [10.1063/1.1315344](https://doi.org/10.1063/1.1315344)
- You, H.; Dai, Y.; Zhang, Z.; Ma, D. *J. Appl. Phys.* **2007**, 101, 026105.
DOI: [10.1063/1.2430511](https://doi.org/10.1063/1.2430511)
- Shen, Y.; Hosseini, A. R.; Wong, M. H.; Malliaras, G. G. *ChemPhysChem*, **2004**, 5, 16.
DOI: [10.1002/cphc.200300942](https://doi.org/10.1002/cphc.200300942)
- Meyer, J.; Hamwi, S.; Bülow, T.; Johannes, H.-H.; Riedl, T.; Kowalsky, W. *Appl. Phys. Lett.* **2007**, 91, 113506.
DOI: [10.1063/1.2784176](https://doi.org/10.1063/1.2784176)
- Nicolai, H. T.; Wetzelaer, G. A. H.; Kuik, M.; Kronemeijer, A. J.; de Boer, B.; Blom, P. W. M. *Appl. Phys. Lett.* **2010**, 96, 172107.
DOI: [10.1063/1.3391668](https://doi.org/10.1063/1.3391668)
- Mauer, R.; Kastler, M.; Laquai, F. *Adv. Funct. Mater.* **2010**, 20, 2085.
DOI: [10.1002/adfm.201000320](https://doi.org/10.1002/adfm.201000320)
- Sirringhaus, H.; Brown, P. J.; Friend, R. H.; Nielsen, M. M.; Bechgaard, K.; Langeveld-Voss, B. M. W.; Spiering, A. J. H.; Janssen, R. A. J.; Meijer, E. W.; Herwig P.; de Leeuw, D. M. *Nature* **1999**, 401, 685-688.
DOI: [10.1038/44359](https://doi.org/10.1038/44359)
- Kaz'ukauskas, V.; Pranaitis, M.; Sicot L.; Kajzar, F. *Mol. Cryst. Liq. Cryst.* **2006**, 447, 141-153.
DOI: [10.1080/15421400500387072](https://doi.org/10.1080/15421400500387072)
- Kim, D. Y.; Subbiah, J.; Sarasqueta, G.; So, F.; Ding, H.; Irfan, Gao, Y. *Appl. Phys. Lett.* **2009**, 95, 093304.
DOI: [10.1063/1.3220064](https://doi.org/10.1063/1.3220064)



A Monthly Journal

Publish your article in this journal

Advanced Materials Letters is an official international journal of International Association of Advanced Materials (IAAM, www.iaamonline.org) published monthly by VBRI Press AB from Sweden. The journal is intended to provide high-quality peer-review articles in the fascinating field of materials science and technology particularly in the area of structure, synthesis and processing, characterisation, advanced-state properties and applications of materials. All published articles are indexed in various databases and are available download for free. The manuscript management system is completely electronic and has fast and fair peer-review process. The journal includes review article, research article, notes, letter to editor and short communications.

Copyright © 2016 VBRI Press AB, Sweden

www.vbripress.com/aml